

On the Effect of an Aggressive Inlet Swirl Profile on the Aero-thermal Performance of a Cooled Vane

*Original*

On the Effect of an Aggressive Inlet Swirl Profile on the Aero-thermal Performance of a Cooled Vane / Insinna, M., Griffini, D., Salvadori, S., Martelli, F.. - In: ENERGY PROCEDIA. - ISSN 1876-6102. - ELETTRONICO. - 81:(2015), pp. 1113-1120. [10.1016/j.egypro.2015.12.133]

*Availability:*

This version is available at: 11583/2760674 since: 2019-10-15T14:56:25Z

*Publisher:*

Elsevier

*Published*

DOI:10.1016/j.egypro.2015.12.133

*Terms of use:*

This article is made available under terms and conditions as specified in the corresponding bibliographic description in the repository

*Publisher copyright*

(Article begins on next page)



69th Conference of the Italian Thermal Engineering Association, ATI 2014

## On the Effect of an Aggressive Inlet Swirl Profile on the Aero-Thermal Performance of a Cooled Vane

Massimiliano Insinna, Duccio Griffini, Simone Salvadori\*, Francesco Martelli

*Department of Industrial Engineering DIEF, University of Florence, via di Santa Marta 3, 50139 Florence, Italy*

---

### Abstract

A high-pressure vane equipped with a realistic film-cooling configuration has been studied. The vane is characterized by the presence of multiple rows of fan-shaped holes along pressure and suction side while the leading edge is protected by a showerhead system. Steady three-dimensional Reynolds-Averaged Navier-Stokes (RANS) simulations have been performed. A preliminary grid sensitivity analysis has been performed (with uniform inlet flow) to quantify the effect of the spatial resolution. Turbulence model has been assessed in comparison with available experiment data. The effects of a realistic inlet swirl on the aero-thermal performance of the cooling system are then investigated by means of comparison between two different kinds of simulations. The first one using a uniform inlet flow while the second one with aggressive swirl derived from the EU-funded project TATEF2. Clocking effects are also accounted for. The effect of the swirling flow in determining the coolant transport are investigated, evidencing the key role that these phenomena have in determining the effectiveness of the cooling.

© 2015 The Authors. Published by Elsevier Ltd. This is an open access article under the CC BY-NC-ND license (<http://creativecommons.org/licenses/by-nc-nd/4.0/>).

Peer-review under responsibility of the Scientific Committee of ATI 2014

*Keywords:* film-cooling, high-pressure vane, swirl, realistic inflow, fan-shaped holes, clocking effects

---

---

\* Corresponding author. Tel.: +39-055-275-8775; fax: +39-055-275-8755.  
*E-mail address:* [simone.salvadori@unifi.it](mailto:simone.salvadori@unifi.it)

**Nomenclature**

$k_T$	Turbulent kinetic energy [ $\text{m}^2/\text{s}^2$ ]
$k_L$	Laminar kinetic energy [ $\text{m}^2/\text{s}^2$ ]
L	Chord [m]
T	Temperature [K]
$y^+$	Non-dimensional wall distance [-]

**Subscripts**

0	Stagnation value
1	Evaluated at the inlet section
2	Evaluated at the outlet section
ax	Axial
aw	Adiabatic wall
c	Coolant
main	Main-flow
rec	Recovery
w	Wall

**Greek**

$\eta$	Effectiveness [-]
$\xi$	Loss coefficient [-]
$\omega$	Specific dissipation rate [1/s]

**1. Introduction**

Numerical simulation of a cooled high-pressure vane is one of the most challenging topics in Computational Fluid Dynamics (CFD). It includes the analysis of a compressible flow with very different geometrical length scales. The usage of Large-Eddy Simulation (LES) for heat transfer analysis in HPV has been documented by Gourdain *et al.* in [1]. A less demanding approach based on the Detached-Eddy Simulation (DES) methodology has been suggested by Takahashi *et al.* [2] in comparison with an Unsteady Reynolds-Averaged Navier-Stokes (URANS) calculation with the  $k-\varepsilon-v^2-f$  transition model by Lien and Kalitzin [3]. However, heat transfer in cooled HPV is usually analyzed considering steady simulations where turbulence is modeled using two-equation approaches. Adami *et al.* [4] demonstrated that the  $k-\omega$  model by Wilcox [5] is able to reproduce the Nusselt number distribution on the blade surface with reasonable accuracy. Insinna *et al.* [6][7] studied the ability of the  $k_T-k_L-\omega$  model by Walters and Cokljat [8] to deal with a realistic film-cooled vane configuration, showing the relevant effect of bypass transition in the Nusselt number evaluation.

To improve the fidelity of the simulations, realistic non-uniform inlet conditions must be included. Swirl motion, enforced by swirlers in the combustor, is conserved up to the entry section of the HPV and convected inside of it, altering aerodynamics and heat transfer, as demonstrated experimentally by Giller and Schiffer [9] and numerically by Pyliouras *et al.* [10] and Salvadori *et al.* [11][12]. The main effect of swirl is to modify the shape of the stagnation line and then the radial distribution of aerodynamic load, leading to an altered pressure ratio across each cooling channel. This could have unexpected consequences if the cooling system is designed with a uniform flow.

The present activity deals with the study of the test rig proposed in [13] and [14]. The aim is to provide an accurate analysis of a heavily cooled high-pressure vane subjected to aggressive inlet swirl and to point out the physical effects that drive coolant migration along the vanes.

## 2. Description of the test case

The test case studied is described by Jonsson and Ott [13] and by Charbonnier *et al.* [14]. It is a transonic research vane experimentally investigated (with uniform inflow) in a linear cascade at the École Polytechnique Fédérale de Lausanne during the TATEF2 European project. The Reynolds number, based on the true chord and evaluated at the outlet section, is about  $1.46E+06$  while the value of the isentropic exit Mach number is about 0.88. The cooling system consists of three rows of fan-shaped holes on both suction and pressure side and four rows of cylindrical holes on the leading edge (showerhead). CO<sub>2</sub> is used as coolant to provide a coolant-to-main-flow density ratio of about 1.6, which is representative of engine-like conditions. More details on the non-dimensional parameters of the cooling system are given in [13]. Operating conditions are summarized in Table 1.

Table 1. Vane boundary conditions

	Main	Coolant	Wall	Outlet
Inlet Total Pressure [bar]	1.535	1.780		
Inlet Total Temperature [K]	333.	303.		
Inlet Turbulence Level [%]	10.	5.		
Inlet Turbulent Length Scale [m]	0.013	0.0004		
Wall Temperature (for isothermal calculations) [K]			323.	
Static Pressure [bar]				0.927

## 3. Numerical approach and simulation matrix

Numerical simulations on hybrid unstructured grids have been performed using a steady approach with the commercial code ANSYS Fluent®. The transitional  $k_T-k_L-\omega$  model by Walters and Cokljat [8] has been selected as a turbulence closure. A second-order accurate upwind discretization has been applied in space, while gradients are reconstructed with the Green-Gauss node based approach. For sake of clarity all the performed simulations are summarized in Table 2. The first part of the work is dedicated to a grid dependence analysis. The second part consists in the examination of the transition model behavior. Finally, the performance of the cooling system has been evaluated in terms of adiabatic effectiveness ( $\eta_{aw}$ ) with uniform and swirled inlet profiles.

Table 2. Simulation matrix.

Type of analysis	Domain	Cooling	Wall thermal condition	n° of runs
Grid sensitivity	Single vane, experimental configuration	Yes	$T_w = 323$ K	4
Turbulence model assessment ( $\eta_{aw}$ )	Single vane, experimental configuration	Yes	$T_w = 323$ K	3
Turbulence model assessment ( $M_{is}$ )	Single vane, experimental configuration	No	$T_w = 323$ K	1
Uniform inlet profile, $\eta_{aw}$	Double vane, reduced aspect ratio	Yes	Adiabatic	1
Swirled inlet profile, $\eta_{aw}$	Double vane, reduced aspect ratio	Yes	Adiabatic	2

The computational domain used for grid sensitivity analysis and turbulence model assessment reproduces the experimental configuration. It includes the whole fluid region including coolant channels and plenum, colored in blue in Fig. 1a. Inlet and outlet sections are placed respectively about  $0.65L_{ax}$  upstream of the leading edge and about  $0.60L_{ax}$  downstream of the trailing edge. The inlet section of the cooling flow is located on top of the cascade. Total pressure, total temperature, turbulence level, turbulent length scale and flow direction have been imposed on inlet sections for all the simulation. Thermal conditions on the surfaces of vane and end-walls are summarized in Table 2.

For the study of the effects of inlet swirl a modified domain, with two passages, has been generated using the same cooling system but with a reduced aspect ratio vane (Fig. 2a). Clocking effects are evaluated using two different vane/swirl alignments, shown in Fig. 2b and referred as “passage aligned” (top) and “LE aligned”

(bottom). The first configuration has the vortex center aligned with the passage while for the second one the alignment is with the leading edge of the vane 2. The swirl profile used for the simulations is the one described by Salvadori *et al.* [11][12].

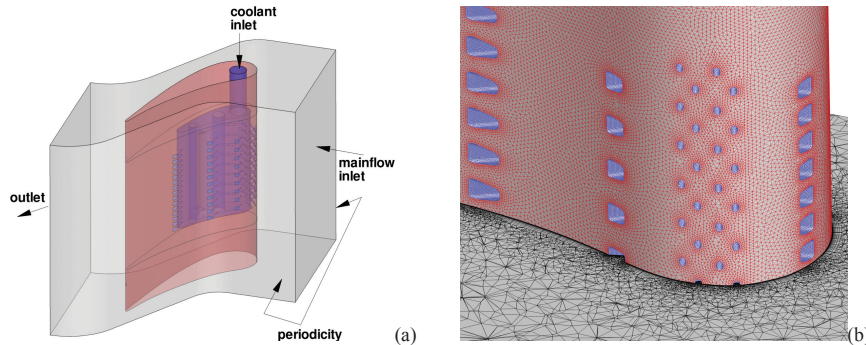


Fig. 1 (a) Schematic of the computational domain (experimental configuration); (b) view of the grid (14.2M elements).

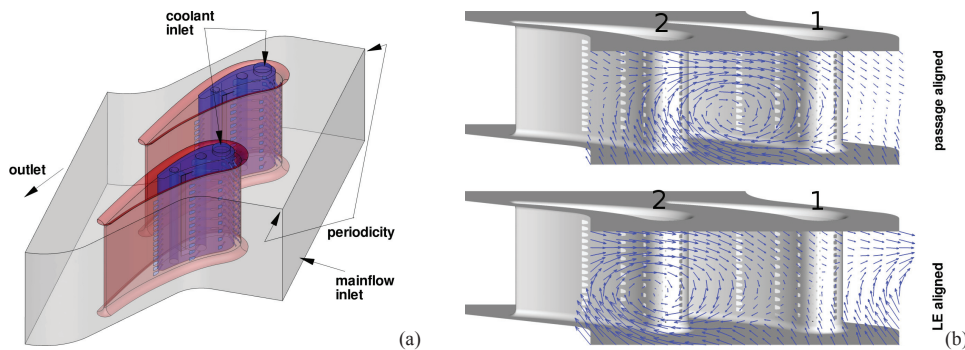


Fig. 2 (a) Schematic of the doubled computational domain; (b) Swirl alignments: passage aligned (top) and LE aligned (bottom).

#### 4. Grid dependence analysis

Hybrid unstructured grids generated with the commercial software Centaur™ have been generated. Prismatic layers are used in the near the walls to reproduce boundary layer while tetrahedral elements fills the remaining volume. Refinements have been enforced in the cooling channels and in the mixing zone between cooling flow and mainstream, as it is possible to observe in Fig. 1b.

Four different grids have been generated consisting of about 3.66M, 6.35M, 14.2M and 25.9M elements. For all the grids the number of prismatic layers and their height are the same, in order to maintain the accuracy in the discretization of boundary layer. For all the cases the average  $y^+$  is about 0.3 while its maximum is about 0.92.

Some results of the grid dependence analysis are shown in Fig. 3. All the grids are almost equivalent in predicting the isentropic Mach number distribution (Fig. 3a), while appreciable differences are present considering the effects on the mass flows shown in Fig. 3b. Values are normalized with respect to the result obtained using the 25.9M mesh. Grid dependence has also been quantified for the mass-flows and total pressure losses using the Grid Convergence Index suggested by Roache *et al.* [15]: the GCI value for coolant mass-flow on the fine mesh is 1.18% while for the loss coefficient (defined in equation (1)) is 0.45%. It can be concluded that increasing the computational cost from 14.2M elements to 25.9M the solution variation is sufficiently low and then the 14.2M grid has been selected for the subsequent simulations.

$$\xi = \frac{P_{01,main} - P_{02}}{P_{02} - P_2} \quad (1)$$

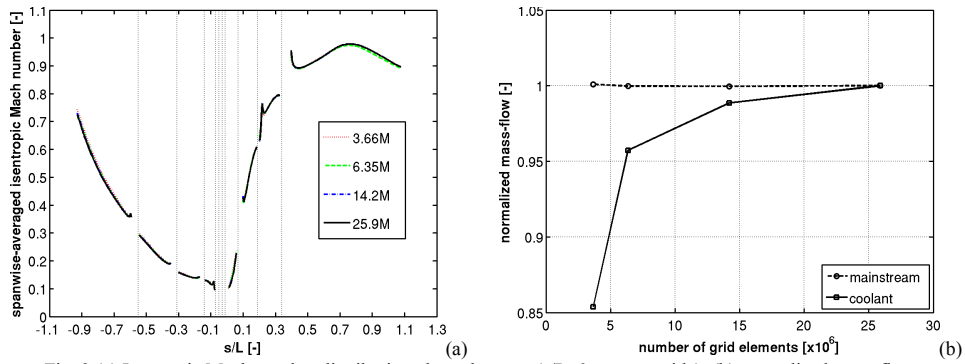


Fig. 3 (a) Isentropic Mach number distribution along the vane ( $s/L < 0$  pressure side); (b) normalized mass-flows.

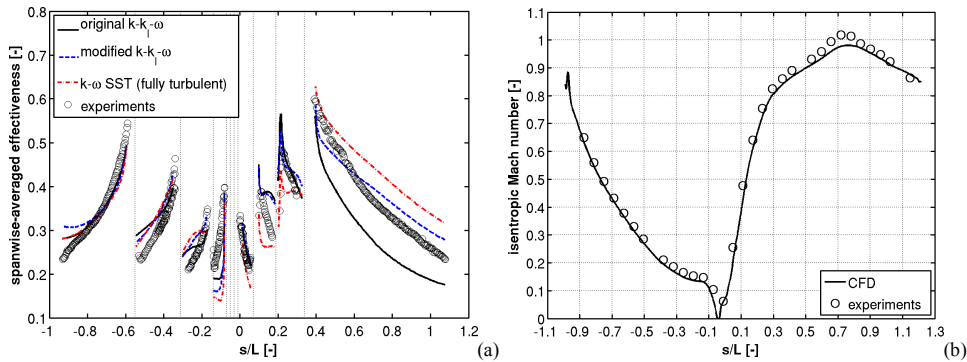


Fig. 4 Comparison of measurements and predictions of: (a) span-wise-averaged adiabatic effectiveness; (b) isentropic Mach number for the uncooled configuration (50% of the span).

### 5. Assessment of the $k_T-k_L-\omega$ model

After selecting the appropriate grid, the assessment of the turbulence model has been performed using the  $k_T-k_L-\omega$  model by Walters and Cokljat [8]. It is based on the  $k-\omega$  structure but is able to predict both natural and bypass transition mechanisms thanks to a third transport equation for laminar kinetic energy  $k_L$  that predicts the behavior of the low-frequency velocity fluctuations in the pre-transitional zones. For the assessment proposed in this work the modified model from the work of Insinna *et al.* [6] has been used. Results, in terms of the span-wise-averaged adiabatic effectiveness (defined in equation (2)) are compared with the available experimental data, with the original model by Walters and Cokljat [8] and with the fully turbulent SST  $k-\omega$  model.

A good agreement is obtained between the qualitative trends of predictions and experiments (Fig. 4a). Comparing the turbulence models, different behaviors are shown downstream of the cooling rows (represented by dotted lines in Fig. 4a). The zone where turbulence models are more discordant is downstream the last cooling row on the suction side ( $s/L > 0.4$ ), where the SST  $k-\omega$  over-predicts  $\eta_{aw}$  while the original  $k_T-k_L-\omega$  significantly under-predicts  $\eta_{aw}$ . In that region the modified  $k_T-k_L-\omega$ , assessed by Insinna *et al.* [6], shows the best performance. Looking also at the other zones, the modified  $k_T-k_L-\omega$  demonstrates to be a good compromise for the prediction of  $\eta_{aw}$ ; it is then used for the subsequent simulations. The distribution of isentropic Mach number at 50% of the span, obtained with the selected turbulence model along the uncooled geometry, is compared with experimental data in Fig. 4b. A general good agreement is obtained, except for  $0.6 < s/L < 0.8$  where the isentropic Mach number is slightly underestimated. The same underestimation has been observed in literature (see [14]) with the SST  $k-\omega$  model.

$$\eta_{aw} = \frac{T_{rec,main} - T_{aw}}{T_{rec,main} - T_{0c}} \tag{2}$$

## 6. Aerodynamic performance

Fig. 5a shows the tangentially-averaged total pressure profiles at the outlet of the vane. The total pressure distribution relative to the passage aligned case evidences reductions with respect to the uniform case at 85% and 15% of the span while, the LE aligned case shows reduction peaks at 85%, 50% and 15%. These are mainly due to the interaction between swirl and secondary flows. Strong swirl effects are also evident comparing swirled cases with the uniform one in terms of tangentially averaged yaw angle at the outlet of the vane (Fig. 5b). The passage aligned case shows overturning from the hub up to 60% of the span and under-turning in the remaining part while LE aligned case shows overturning from the hub to the 32% of the span and under-turning in the remaining part. The extreme values of under-turning and overturning are reached respectively at 83% of the span for the passage aligned case ( $-3.4^\circ$ ) and at 6% of the span for the LE aligned case ( $+5.2^\circ$ ). These changes could lead to unexpected loads of the rotor blades if not appropriately taken into consideration during design process.

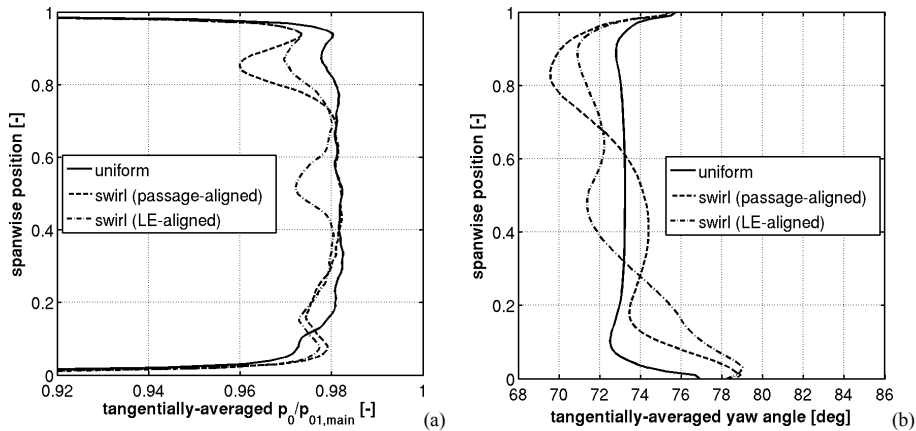


Fig. 5 Tangentially averaged quantities at the vane outlet: (a) non-dimensional total pressure; (b) yaw angle.

## 7. Adiabatic effectiveness

In this section, the adiabatic effectiveness of the cooling system (it has been previously defined in equation 1 but this time is calculated using  $T_{01}$  instead of the  $T_{rec,main}$ ) is analyzed. Results for the doubled vane with uniform and swirled conditions are shown in Fig. 6. Uniform simulation shows a good overall covering effect of the film cooling system even if low effectiveness is present at the leading edge in the shroud region due to the downward angle of the showerhead holes. Consequently, a jet impinges the lower end-wall generating an advantage for its coverage.

Swirling cases show three main effects on the adiabatic effectiveness. The first one is the effect of the main-flow incidence variation along the leading edge. This affects mainly showerhead behavior since the external pressure field is modified, leading to performance deterioration with respect to the uniform case. The second effect is that, despite the showerhead low efficacy, the modified working conditions imply a beneficial effect for the hub, which is partially covered by the jets coming from the showerhead itself, especially near the pressure side. The third effect is due to swirl migration and its interaction with cooling jets and secondary flows (enforcing lower passage vortex and suppressing higher). For the passage aligned case, Fig. 6 (c-d), the swirl is convected inside the central passage thus affecting mainly the pressure side of the vane 1 and suction side of the vane 2, with detrimental effects respectively over the mid-span and under the mid-span. For the LE aligned case, Fig. 6 (e-f), the vortex core is convected in the other passage thus affecting vane 2 pressure side and vane 1 suction side showing similar detrimental effects previously highlighted.

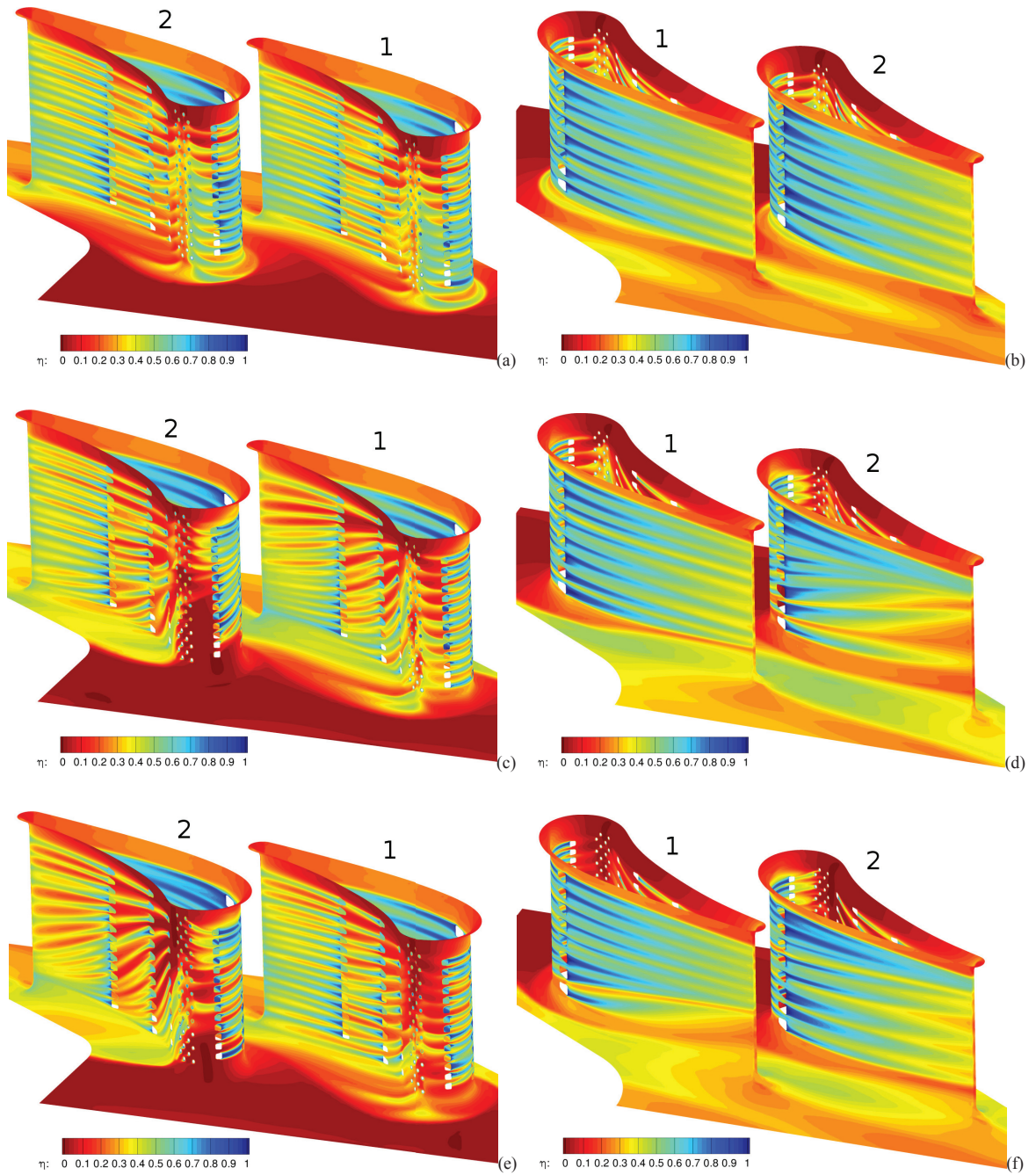


Fig. 6 Adiabatic effectiveness distributions for: (a-b) the uniform inlet case; (c-d) passage aligned case; (e-f) LE aligned case.

## 8. Concluding remarks

Aerodynamics and film cooling effectiveness of a high-pressure turbine vane have been analyzed by means of steady RANS simulations. After grid sensitivity study and turbulence model assessment the effects of an inlet swirl have been investigated taking into account two clocking positions. Results, compared with a uniform inlet case, have shown that inlet swirl is detrimental in terms of vane coverage, in particular from the point of view of the showerhead. The convection of vortex cores inside passages and their consequent interaction with secondary flows determines remarkable modifications of the coolant coverage with respect to the uniform inlet case. This lead to state that residual swirl motion must be considered during the design phase of the cooling system in order to guarantee reliability of the components when subjected to the machine working conditions.

## Acknowledgements

The European Commission and the Turbine Aero-Thermal External Flows 2 (TATEF2) consortium (FP6 project, contract no. AST3-CT-2004-502924) are acknowledged.

## References

- [1] Gourdain N, Gicquel LYM, Collado E. Comparison of RANS simulation and LES for the prediction of heat transfer in a highly loaded turbine guide vane. Proc. of the Ninth European Conference on Turbomachinery – Fluid Dynamics and Thermodynamics 2011, March 21-25, Istanbul, Turkey.
- [2] Takahashi T, Funazaki K, Salleh HB, Sakai E, Watanabe K. Assessment of URANS and DES for prediction of leading edge film cooling. J Turbomach 2012, 134.
- [3] Lien FS, Kalitzin G. Computations of transonic flow with the  $v^2$ - $f$  turbulence model. Int. J. Heat Fluid Flow 2001, 22(1): 53–61.
- [4] Adami P, Martelli F, Chana KS, Montomoli F. Numerical predictions of film cooled NGV blades. Proc. of IGTI, ASME Turbo Expo 2003 June 16-19, Atlanta, Georgia, USA, Paper No. GT-2003-38861.
- [5] Wilcox DC. Turbulence Modeling for CFD. DCW Industries Inc. 1993.
- [6] Insinna M, Griffini D, Salvadori S, Martelli F. Film cooling performance in a transonic high-pressure vane: decoupled simulation and conjugate heat transfer analysis. Energy Procedia, 45, 2014, pp. 1126-1135, doi: 10.1016/j.egypro.2014.01.118.
- [7] Insinna M, Griffini D, Salvadori S, Martelli F. Conjugate heat transfer analysis of a film cooled high-pressure turbine vane under realistic combustor exit flow conditions. In: Proc. of the ASME Turbo Expo 2014, Dusseldorf, Germany, June 16-20, Paper No. GT2014-25280
- [8] Walters DK, Cokljat D. A three-equation eddy-viscosity model for Reynolds-averaged Navier-Stokes simulations of transitional flow. J Fluids Engineering 2008. 130(4).
- [9] Giller L, Schiffer H. Interactions between the combustor swirl and the high pressure stator of a turbine. Proc. of IGTI, ASME Turbo Expo 2012, June 11-15, Copenhagen, Denmark, Volume 8: Turbo Expo 2012, Paper No. GT-2012-69157, pp. 1401-1415, doi: 10.1115/GT2012-69157.
- [10] Pylouras S, Schiffer H, Janke E, Willer L. Effects of non-uniform combustor exit flow on turbine aerodynamics. In: Proc. of the ASME Turbo Expo 2012: Turbine Technical Conference and Exposition, Volume 8: Turbomachinery, Parts A, B, and C, Copenhagen, Denmark, June 11-15, pp. 1691-1701, doi: 10.1115/GT2012-69327.
- [11] Salvadori S, Ottanelli L, Jonsson M, Ott P, Martelli F. Investigation of high pressure turbine endwall film cooling performance under realistic inlet conditions. AIAA Journal of Propulsion and Power, Vol. 28, Issue 4, August 2012, pp. 799-810, doi: 10.2514/1.59225.
- [12] Salvadori S, Riccio G, Insinna M, Martelli F. Analysis of combustor/vane interaction with decoupled and loosely coupled approaches. In: Proc. of the ASME Turbo Expo 2012: Turbine Technical Conference and Exposition, Volume 8: Turbomachinery, Parts A, B, and C, Copenhagen, Denmark, June 11-15, pp. 2641-2652, doi: 10.1115/GT2012-69038.
- [13] Jonsson M, Ott P. Heat transfer experiments on a heavily film cooled nozzle guide vane. Proc. of the Seventh European Conference on Turbomachinery – Fluid Dynamics and Thermodynamics 2007, pp. 1011-1020, March 5-9, Athens, Greece.
- [14] Charbonnier D, Ott P, Jonsson M, Köbke T, Cottier F. Comparison of numerical investigations with measured heat transfer performance of a film cooled turbine vane. Proc. of the ASME Turbo Expo 2008: Power for Land, Sea, and Air, Volume 4: Heat Transfer, Parts A and B, Berlin, Germany, June 9–13, pp. 571-582, doi: 10.1115/GT2008-50623.
- [15] Roache PJ, Kirti NG, White FM. Editorial policy statement on the control of numerical accuracy. J. Fluids Eng. 108, pag. 2, doi: 10.1115/1.3242537